Bioprocess and Biosystems Engineering (2019) 42:1215–1224
https://doi.org/10.1007/s00449-019-02119-4

RESEARCH PAPER

Embedding live bacteria in porous hydrogel/ceramic nanocomposites for bioprocessing applications

Jessica Condi Mainardi[1] · Kurosch Rezwan[1,2] · Michael Maas[1,2]

Received: 2 November 2018 / Accepted: 29 March 2019 / Published online: 5 April 2019

Abstract

In this work, we present a biocompatible one-pot processing route for ceramic/hydrogel nanocomposites in which we embed live bacteria. In our approach, we fabricate a highly stable alginate hydrogel with minimal shrinkage, highly increased structural and mechanical stability, as well as excellent biocompatibility. The hydrogel was produced by ionotropic gelation and reinforced with alumina nanoparticles to form a porous 3D network. In these composite gels, the bacteria *Escherichia coli* and *Bacillus subtilis* were embedded. The immobilized bacteria showed high viability and similar metabolic activity as non-embedded cells. Even after repeated glucose consumption cycles, the material maintained high structural stability with stable metabolic activity of the immobilized bacteria. Storing the bionanocomposite for up to 60 days resulted in only minor loss of activity. Accordingly, this approach shows great potential for producing macroscopic bioactive materials for biotechnological processes.

Keywords Cell encapsulation · Nanocomposite · Hydrogel · Ceramic nanoparticles

Introduction

Immobilizing bacteria or other microorganisms inside semi-permeable substrates can be desirable for biotechnological processes like wastewater treatment [1–3], fermentation of sugars [4–7] or manufacturing of nutritional [8] and pharmaceutical products [9, 10]. However, embedding living microorganisms in artificial materials necessitates the use of both biocompatible starting materials as well as fully biocompatible processing steps. For that reason, bacteria are frequently encapsulated in hydrogel microspheres for use in bioreactors. Immobilization of bacteria in hydrogel microspheres or similar designs simplifies the process of separation and purification, since the microspheres can be easily separated from the solution, reducing costs and processing time [11–14]. Furthermore, immobilized bacteria are more strongly protected from toxic substances and adverse surroundings and were shown to exhibit higher activity under some circumstances [15, 16]. Alginates in particular are widely used for microorganism immobilization because of their biocompatible gelation reaction, which takes place at room temperature and at physiological pH [17–19]. However, alginate hydrogels can hardly meet the mechanical requirements for the harsh conditions that are often present in bioreactors [20]. Furthermore, the fabrication of complex shapes with a combination of advanced material properties like macro-porosity and structural stability is difficult to achieve with soft polymer gels.

The ionotropic gelation of alginate is based on cross-linking the anionic polymer with divalent and polyvalent cations, such as Ca^{2+} [21]. External gelation, which is widely used for cell encapsulation inside microspheres, usually describes the process of dropping an aqueous alginate solution into an aqueous calcium chloride ($CaCl_2$) solution, resulting in fast gelation of the drop from its outside towards the inside [22].

Electronic supplementary material The online version of this article (https://doi.org/10.1007/s00449-019-02119-4) contains supplementary material, which is available to authorized users.

✉ Michael Maas
michael.maas@uni-bremen.de

Jessica Condi Mainardi
mainardi.jessica@uni-bremen.de

Kurosch Rezwan
krezwan@uni-bremen.de

[1] Keramische Werkstoffe und Bauteile, Advanced Ceramics, Universität Bremen, Am Biologischen Garten 2-IW 3, Raum 2140, 28359 Bremen, Germany

[2] MAPEX Center for Materials and Processes, University of Bremen, Am Fallturm 1, 28359 Bremen, Germany

For cell encapsulation, this established approach ensures sufficient stability for the gel and thereby high cell protection. However, this method results in an inhomogeneous hydrogel matrix due to the cation diffusion gradient established from the non-gelled center toward the boundaries. This inhomogeneity can delay solute exchange, specifically diffusion of nutrients into and toxic metabolic waste from the bead [23, 24]. In contrast, internal gelation describes the pH-controlled dissociation of an insoluble salt, such as calcium carbonate, which is distributed inside the gel matrix, resulting in controlled and slow release of Ca^{2+} ions. Enhanced control over the gelation process enables a more homogeneous gel structure. Compared to external gelation, internal gelation results in a weaker gel matrix with lower encapsulation efficiency, but it improves solute exchange [22, 23]. Internal gelation allows designing specific gel morphologies and fine control over matrix density.

To overcome common limitations of hydrogels, several strategies focus on hybrid materials consisting of combinations of hydrogels and inorganic materials [25–27]. In this respect, ceramic nanoparticles like alumina are widely known for their high hardness, chemical inertness and high biocompatibility [28, 29]. The combination of organic and inorganic materials can enhance a range of properties, resulting in the emergence of unique and novel features [30]. However, producing a nanocomposite hydrogel with mechanical stability and bioactivity is still a challenge [31, 32]. Mainly, the presence of living microorganisms restricts some processing routes and parameters, since cell survival requires mild pH, moderate temperature and low shrinkage of the composite matrix. Furthermore, it is essential that nutrients are able to reach the microorganisms inside the material.

Similarly, immobilization of living cells has also been pursued with inorganic porous materials [33, 34]. To this end, Pannier et al. used the sol–gel process for the synthesis of silica gels by adapted freeze casting with immobilized microorganisms. The main advantage of this technique lies in the generation of highly mechanically stable materials with high open porosity [35]. However, direct contact of cells with silica precursors during synthesis as well as the freezing and thawing cycles during freeze casting can be detrimental for biological entities [34]. To mitigate this effect, a two-step procedure was developed by Perullini et al. which starts with pre-encapsulation of *Bacillus subtilis* spores and *Escherichia coli* in calcium alginates beads, followed by silicate polymerization, leading to a nanoporous monolithic structure with embedded bacteria [36, 37]. This strategy was also shown to enable material processing in an extended range of pHs, since the cells are more strongly protected by the polymer. However, even if the biocompatibility increases, metal alkoxides used for the sol–gel technique cannot be considered to be fully biocompatible due to the harsh process conditions and associated release of alcohols [33, 38].

This study aims to develop a biocompatible strategy for synthesizing ceramic/hydrogel nanocomposites in which live bacteria can be embedded. Several factors can potentially influence the viability of embedded cells, such as preparation conditions, type of cell, residual water content, storage conditions [16] and accessibility of nutrients. Furthermore, a matrix with structural rigidity assures stability of both the overall material as well as of the pore structure. For this reason, we developed a straightforward one-pot processing route based on the reinforcement of an alginate hydrogel with alumina nanoparticles, followed by the addition of bacteria and subsequent internal/external ionotropic gelation steps. The immobilization of Gram-negative (*E. coli*) and Gram-positive (*B. subtilis*) model bacteria in an alginate structure during gelation is expected to provide a suitable environment for bacteria, since this structure possesses high water content and good biocompatibility. Moreover, alumina nanoparticles are used as a reinforcement to increase structural stability of the porous hydrogel matrix while shrinkage is reduced. All bionanocomposites are characterized concerning their pore window size, open porosity, shrinkage and water content. Compression tests are performed to determine the influence of alumina nanoparticles and the gelation process on structural stability. Furthermore, bacterial viability and activity inside the composites is determined by measuring glucose consumption over time and the long-term performance and stability of the bionanocomposites are also characterized.

Materials and methods

Chemicals

The alumina powder was purchased from Almatis (CT 3000 SG, d_{50} = 500 nm, Lot.: 1146370986 purity 99.78%). Calcium carbonate (Product Number: 795445, Lot.: MKBW4839V), gluconic acid (Product Number: G1951, Lot.:BCBQ7487V), glucose (Product Number: G8270, Lot.: SZBF0820V), alginic acid sodium salt from brown algae—medium viscosity (Product Number.: A2033, Lot.: SLBR0395V), PBS (Product Number: P4417, Lot.: SLBG2698V), calcium chloride dehydrate (Product Number: 21102, Lot.: BCBM5521V), LB broth (Product Number: L3022, Lot.: BCBS9423) and glutaraldehyde solution (Product number: G5882, Lot.: SLBL7631V) were purchased from Sigma-Aldrich Chemie GmbH, Germany. The second alginate Protanal LFR 5/60 Sodium Alginate (Lot.: H192104) was obtained from FMC Biopolymer (Philadelphia, USA) and the enzymatic assay used for determination of glucose concentration in solutions was Glucose

Liquicolor (Product number.: 10121, Lot.: 0168) from HUMAN, Germany.

Suspension preparation

The slurry was prepared based on Brandes et al. [39] but in sterile conditions. A mixture of both alginates was dissolved in 50 mL Millipore water at room temperature (RT) via a dispermat (IKA RW20.n, Staufen, Germany) for 30 min at 600 rpm. After dissolving the alginates, the alumina powder was slowly added to the prepared alginate-containing aqueous suspension under continuous stirring at 1200 rpm for 30 min at RT, resulting in agglomerate-free alumina slurry with 40 vol% of ceramic particles. The slurry could directly be used for bionanocomposite formation or stored in a refrigerator at 4 °C for up to 3 weeks.

Bacteria strain and culture conditions

The bacterial strain *E. coli* K12 (DMS 1077) and *B. subtilis* (DMS 1088) were set to grow in sterile Lysogeny broth (LB) medium at 37 °C under agitation at 150 rpm in an incubator (Heidolph Unimax 1010). Cells were centrifuged at 2500 rpm for 10 min to obtain the cell pellet. After that, the supernatant was mixed with PBS until the desired concentration of approx. 32.5×10^8 cfu/mL of *E. coli* and 15×10^8 cfu/mL of *B subtilis*, based on McFarland standards.

Bionanocomposite production

After removal from storage at 4 °C, the suspensions were stirred for 5 min at 1200 rpm in sterile conditions, followed by the addition of calcium carbonate salt ($CaCO_3$) (Fig. 1). To test the effect of nutrient addition during bionanocomposite processing, two different compositions were produced: with LB medium and without. Therefore, for the samples with LB medium, 2 mL of the sterile nutrient solution was added in this step to the slurry, before the bacteria. After the suspension was homogenized by stirring, stirring velocity was decreased to 400 rpm and the bacteria solution in PBS was added to the mixture, followed by intense stirring at 1000 rpm for 30 s. Thereafter, gluconic acid was added into the dispersion to initiate the internal cross-linking. Gluconic acid (GLA) dissociates calcium carbonate, releasing calcium cations which are then able to cross-link alginate. A molar ratio of 1:2 $CaCO_3$:GLA was used to maintain a neutral pH value [40, 41]. This suspension was mixed at 1200 rpm for 20 s. Subsequently, the suspension was cast at RT into small petri dishes (⌀ 35 mm), which were covered and half closed with Parafilm to avoid drying, and stored in an incubator at 37 °C for 24 h. After 24 h, the samples were removed from the incubator and directly tested or further stored in a refrigerator at 4 °C. The external gelation was performed just before the glucose uptake experiments to increase structural stability. The samples were submerged separately in a sterile 0.1 M $CaCl_2$ solution for 30 min. After that, the samples were rigorously washed in PBS and were dried for 20 min.

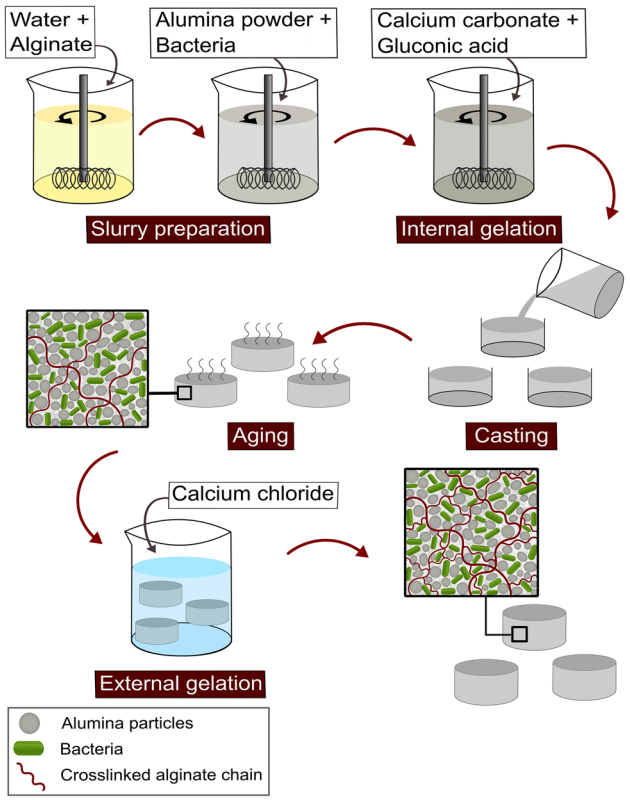

Fig. 1 Scheme illustrating the bionanocomposite processing route based on ionotropic gelation. First, the alginates are dissolved in water followed by the addition of alumina powder. After homogenization of the mixture, microorganisms can be incorporated into the suspension and thereafter internally gelled and cast. To assure sample mechanical stability, an external gelation was performed before the samples were tested

Structural characterization

To characterize the bionanocomposite structure, the samples were dehydrated by a graded series of ethanol (35, 50, 70, 80, 90, 95, 100, 100, and 100% for 10 min each). Thereafter, they were let to dry for 2 days at room conditions. The dry samples were analyzed by mercury intrusion (Pascal 140 and 440, Porotec) to analyze its porosity and pore size. Furthermore, the stability of the material was measured indirectly by determining the weight loss of the composites after a certain time in PBS buffer or water, with and without external gelation, at a temperature of 37 °C and 140 rpm in an incubator.

Mechanical characterization

Eight types of cylindrical samples were prepared: alginate with internal gelation, alginate with internal/external gelation, nanocomposite with internal gelation and nanocomposite with internal/external gelation. The proportion diameter:length was set between 1:1 and 1:1.5. The tests were performed in an universal testing machine (Zwick/Roell Z005) and a half sphere was positioned on the sample to assure that the force was uniformly applied in the whole sample (Fig. 2). The surfaces in contact with the sample were covered with a thin layer of oil (WD-40), to reduce the effect of friction between the gel and the machine during the compression test. Since these materials have high elastic properties, the cross-section will increase with the application of the force. Therefore, the cross-sectional area must be corrected to obtain reliable compressive strength results using the following equation:

$$A_C = \frac{A_0}{1-\varepsilon},$$

where A_C is the corrected area, A_0 is the initial area and ε is the strain, which is defined as a quotient of the variation of high L and initial high L_0 ($\varepsilon = \frac{\Delta L}{L_0}$). After knowing the correct area of the cross-section, it is possible to calculate the compression strength ($\sigma_{comp.}$) using: $\sigma_{comp.} = \frac{F}{A_C}$.

The elastic modulus of these materials was calculated from the slope of the stress vs. strain curves.

Viability test

Bacteria viability was measured with Alamar Blue assay, which is based on the dye resazurin. Viable cells with active metabolism can reduce resazurin into resorufin which is pink and fluorescent. The product can be quantified either by absorbance or fluorescence, where fluorescence is more precise. For that, three replicates of nanocomposites containing *B. subtilis* or *E. coli* (with and without LB medium) were incubated for 2.5 h and for 4 h, respectively, at 37 °C and 100 rpm in a solution of PBS with 10% of Alamar Blue.

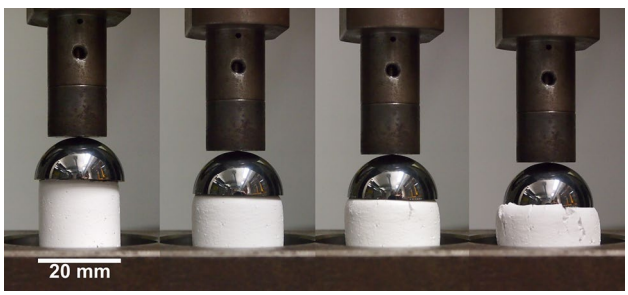

Fig. 2 Compression test of the nanocomposite

Thereafter, bacteria viability was determined by measuring fluorescence at ex. 544 nm and em. 590 nm. To quantify the number of active cells in the bionanocomposites, the same experiment was performed with different known concentrations of freely suspended bacteria and calibration curves were obtained. Controls of nanocomposites without bacteria and freely suspended bacteria viability after 24 h at 37 °C in PBS, to compare with the composites, were tested as well. To confirm bacterial viability, bionanocomposites were cut in small pieces and stained with SYTO 9 and propidium iodide (live/dead staining) for 20 min, protected from light. Thereafter, these samples were analyzed in fluorescence microscope (AXIO from Zeiss).

Glucose consumption measurements

The samples were positioned inside a chamber of a six-well plate directly after the external cross-linking, which was afterwards filled with 3 mL of sterile glucose solution, with an initial concentration of 1 mg/mL. These plates were covered and partially closed with Parafilm, to ensure oxygen diffusion into the chamber. Three replicates from different suspension batches of nanocomposite containing *E. coli*, *E. coli* with LB medium, *B. subtilis* and *B. subtilis* with LB medium were tested. Controls containing freely suspended bacteria and nanocomposites without bacteria were also tested. Samples in contact with the glucose solution were incubated in the six-well plate in a shaker at 37 °C and 140 rpm and the glucose concentration was measured each hour for 24 h. Small amounts (7.5 µL) of the solution were taken out each hour and were mixed with the enzymatic assay Glucose Liquicolor in a 96-well plate. The absorbance was measured at 500 nm to define the glucose concentration. This procedure was the same as used for the cyclic and storage tests. In the case of the cyclic tests, the samples were rigorously washed with PBS after each cycle (24 h) to remove free bacteria and remaining glucose. Subsequently, the bionanocomposites were dried for 20 min and then transferred into fresh glucose media, with a concentration of 1 mg/mL. This procedure was repeated until less than 50% of glucose was consumed. For the storage test, three samples from different batches were removed from refrigerator every 5 days and tested for 24 h, up to day 60. The samples were not submersed in buffer solution during storage.

Results and discussion

Structural characteristics

The ceramic/hydrogel nanocomposites were prepared in small petri dishes ($d = 35$ mm) which defined their cylindrical shape (Fig. 1). Alumina particles, which are positively

Table 1 Structural properties of the bionanocomposite

Bionanocomposite	Porosity (%)	Pore window size (μm)	Shrinkage (vol.%)	Water content (vol.%)
Without bacteria	46 ± 1.2	0.14 ± 0.01	7.4 ± 0.9	54 ± 0.8
With *E. coli*	49 ± 4.8	0.13 ± 0.01	7.9 ± 0.7	53 ± 0.7
With *B. subtilis*	50 ± 1.7	0.14 ± 0.01	6.9 ± 0.9	55 ± 0.8

charged at physiological pH, electrostatically interact with alginate chains, which are negatively charged. The alginate/particle suspension was afterwards cross-linked with Ca^{2+} cations and the combination of these interactions resulted in white composite gels which maintained their overall shape and could be handled without damage for the successive tests. The composites were dehydrated by a graded series of ethanol to characterize porosity and pore size, while different samples were dried at room conditions and their weight loss was measured to define shrinkage and water content (Table 1). Here, an open porosity of around 46% with a pore window size of 0.14 μm was observed. Additionally, the wet sample contained ca. 54 vol.% of internal water and showed a shrinkage of ca. 7.4% after aging. Samples containing the bacteria *E. coli* or *B. subtilis*, which we call in this study bionanocomposite, were also prepared and characterized. The bionanocomposites did not show any significant change in water content, shrinkage or pore size. However, the porosity slightly increased with both bacteria, which might be related to the bacteria population.

Long-term material stability was indirectly measured by determining the weight loss of the composites after a certain time in PBS buffer or water, with and without external gelation, at a temperature of 37 °C and 140 rpm. These results are shown in Figure S1 (supplementary information). The stability of nanocomposites without external gelation incubated in PBS was stable for less than 24 h. External gelation could extend the stability of the nanocomposites which were completely degraded after 9 days. This low stability of alginate in PBS was noted by several authors [42–45] as a result of calcium exchange with buffer ions, resulting in the decalcification of the gel and consequently destabilization. No significant degradation was observed with the nanocomposites submersed in water. Overall, the long-term stability of the samples was sufficient compared to the lifetime of the encapsulated bacteria under real experimental conditions.

Mechanical properties

The mechanical properties of hydrogels can be a critical limitation for these materials in different applications. Here, the composites were initially produced via internal gelation followed by a second cross-linking (external gelation) to achieve sufficient mechanical strength. For mechanical testing, the samples were first submerged in 0.1 M $CaCl_2$ solution for 30 min. Compression tests were performed to evaluate the influence of the gelation steps as well as the mechanical reinforcement of the hydrogel by the addition of ceramic nanoparticles.

Table 2 Compressive strength and elastic modulus of the hydrogel after internal gelation and after the combination of internal and external gelation, with and without the addition of ceramic particles

	Compressive strength (kPa)	Elastic modulus (kPa)
Alginate internal gelation	33.9 ± 5.0	1.5 ± 0.3
Alginate internal/external gelation	44.6 ± 3.7	1.7 ± 0.1
Nanocomposite internal gelation	59.4 ± 2.6	3.6 ± 0.2
Nanocomposite internal/external gelation	132.2 ± 5.8	8.4 ± 0.3

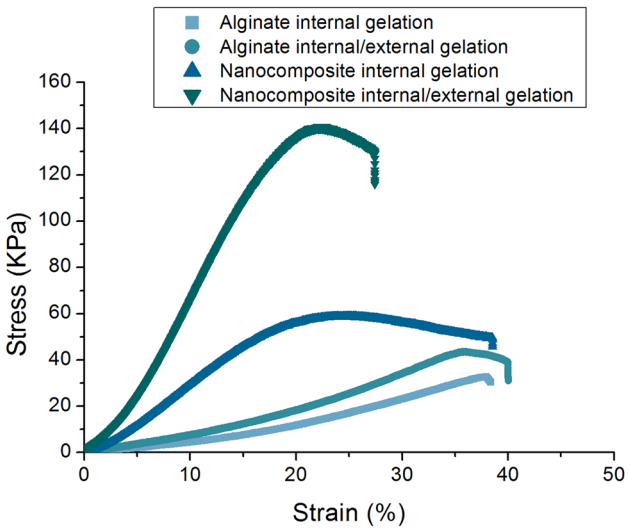

Fig. 3 Compression test of the cylindrical samples showing the influence of the reinforcement and combination of internal and external gelation of the gel on the compression strength

The compressive strength and the elastic modulus (Young's modulus) of the bacteria-free hydrogel after internal gelation and after the combination of internal and external gelation, with and without the addition of ceramic particles are presented in Table 2 and Fig. 3. Internally gelled alginate hydrogels are capable of high deformation

(approx. 40%), but this material shows low elastic modulus (1.5 ± 0.3 kPa) and fails at low compressive strength (33.9 ± 4.9 kPa). A subsequent external gelation resulted in a similar elastic modulus (1.7 ± 0.1 kPa) and a slightly higher compressive strength (44.6 ± 3.7 kPa). This means that the gel matrix, with or without external gelation, can be easily deformed but does not support high compressive strength. However, adding alumina nanoparticles to the internally gelled composite increased the elastic modulus twofold (3.6 ± 0.2 kPa), resulting in a stiffer material. This material reached the maximum compressive strength (59.4 ± 2.6 kPa) at smaller deformation (approx. 20%). After reaching maximum strength, the material started to fail and deformed up to 40%. The compressive strength of the hydrogel/ceramic composites increased to 132.9 ± 5.8 kPa with a subsequent external gelation. Moreover, external gelation increased the elastic modulus to 8.4 ± 0.3 kPa and the material failed at lower deformation (approx. 20%). The combination of internal and external gelation with alumina nanoparticles, which are only electrostatic interactions, reinforced the compressive strength by a factor of about four and also increased elastic modulus six times. This strong structural reinforcement might be caused by the interaction between ceramic particles and polymer chains, which might facilitate the diffusion of Ca^{2+} into the composite during external gelation, cross-linking the inner parts of the composite beyond the surface.

Bacteria viability

Bacterial activity can be observed in all bacteria-containing samples, while negative controls did not show any significant levels of resorufin (Fig. 4, see also Figure S2). For both *E. coli*- and *B subtilis*-containing samples, we observe that only approximately 10% of bacteria were still viable after biocomposite processing. However, after initial processing, the samples were kept in an incubator for 24 h before testing for aging. This period of time could have been detrimental for the bacteria even without any material processing. Therefore, freely suspended bacteria viability was measured after 24 h to determine the influence of the storage time on bacteria viability. For that, bacteria were kept in an incubator for 24 h in PBS solution. The aging reduced approx. 15% of *E. coli* viability and 85% *B. subtilis* viability. Based on these results, freely suspended *B. subtilis* and the bionanocomposite containing the same bacteria showed similar viability, which indicates that the material processing itself might not have strongly influenced *B. subtilis* viability. However, opposite behavior was observed with *E. coli*. In this case, encapsulated *E. coli* showed approx. 80% less viable cells than freely suspended bacteria after 24 h, showing that the processing was more detrimental for *E. coli*.

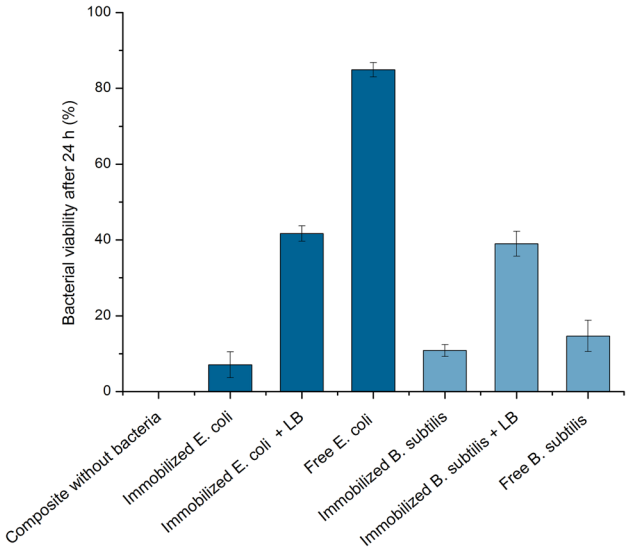

Fig. 4 Viability test of embedded *E. coli* (**a**) and *B. subtilis* (**b**) and freely suspended bacteria after 24 h at 37 °C in comparison to initial bacterial concentration. The influence of additional nutrients (LB medium) on the bionanocomposite was also analyzed

The effect of addition of LB medium during nanocomposite processing on bacteria viability was also analyzed. Here, LB medium increased cell viability in a factor of approx. 5.8 ± 0.29 for *E. coli* and 3.6 ± 0.3 for *B. subtilis*. The nutrients provide a suitable environment and supply the cells during the aging. The differences between *E. coli* and *B. subtilis* are related to the specific metabolism characteristics from each microorganism. These differences also highlight the importance of working with model bacteria of the two different groups.

Influence of immobilization on bacterial metabolism

The immobilization of bacteria in an inorganic structure protects them by preventing direct contact with the potentially harmful environment. However, the structure can also hinder nutrients from reaching the cell, leading to cell death. Therefore, glucose consumption of the embedded cells was measured to determine if the bacteria were active and accessible inside the bionanocomposite. For that, three replicates of different batches were tested to evaluate the performance of *E. coli* and *B. subtilis*, free and immobilized, as well as a negative control without bacteria towards their ability to consume glucose, which is a simple indicator for bacterial viability. These samples were incubated for 24 h and the glucose concentration was measured each hour (Fig. 5).

As shown on Fig. 4, all samples showed some reduction in glucose concentration. Samples containing immobilized *E. coli* or *B. subtilis*, as well as freely suspended bacteria,

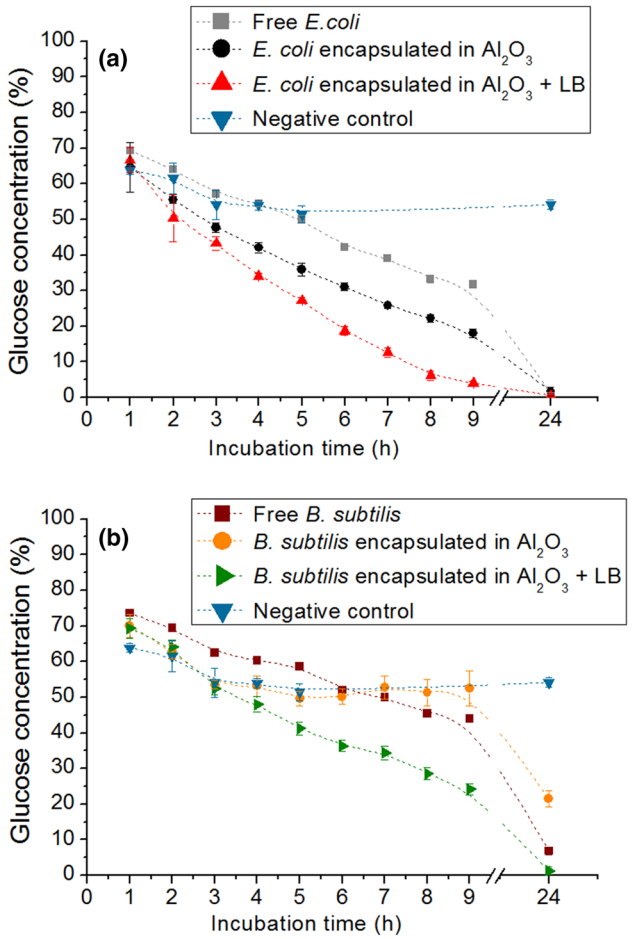

Fig. 5 Glucose uptake from freely suspended and embedded *E. coli* (**a**) and *B. subtilis* (**b**) as a function of time. The influence of additional nutrients (LB medium) on the bionanocomposite was also analyzed

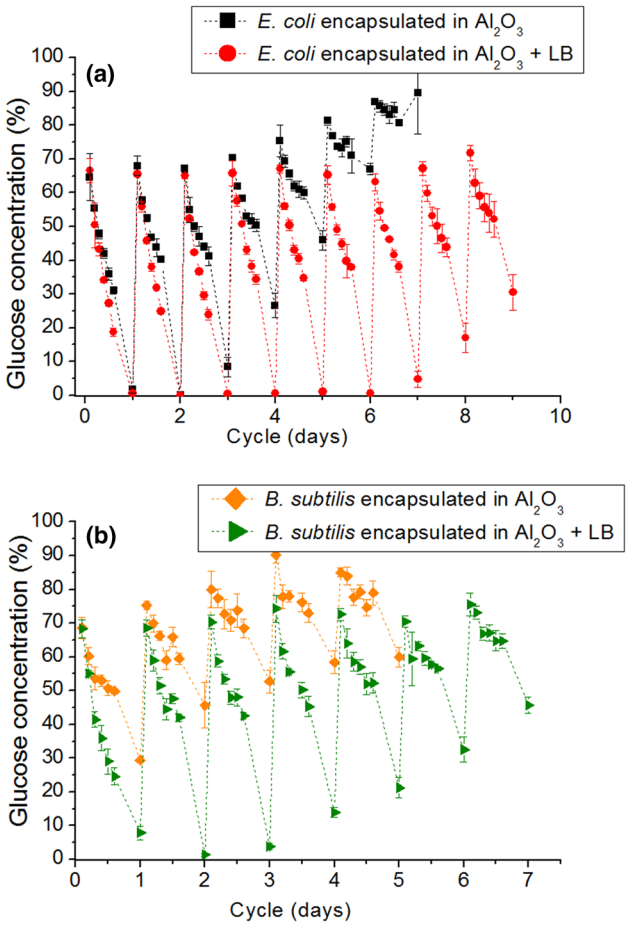

Fig. 6 Long-term performance of bionanocomposites with embedded *E. coli* (**a**) and *B. subtilis* (**b**) with and without the addition of LB medium during several cycles, measured by the glucose concentration over time. Each cycle represents 24 h

exhibited an almost linear glucose consumption over incubation time. Comparing the consumption curves for *E. coli* and *B. subtilis*, it is possible to observe a higher inclination of the curve for *E. coli*, which corresponds to a higher glucose consumption. However, the negative control without bacteria also showed a slight reduction of glucose concentration. This might be related to the residual internal water content (approx. 54 vol.%) of the nanocomposites, which were never completely dried to ensure the survival of the embedded bacteria. In the absence of bacteria, dilution of glucose into the water inside the nanocomposite might occur, resulting in the observed initial reduction of the glucose concentration. However, with samples containing bacteria, only small amounts (or no glucose for *E. coli*) were detected after 24 h. Nevertheless, encapsulated bacteria showed a higher glucose uptake than free bacteria at comparable bacteria concentrations. This observation might again be related to the internal water content of the samples, which dilutes the glucose in the surrounding medium. Considering this, the behavior of the free and encapsulated *E. coli* is similar, with nearly parallel consumption curves.

Additionally, the effect of the addition of nutrients in the form of LB medium during production of the bionanocomposite was analyzed. The addition of the LB medium resulted in a higher glucose uptake for both bacteria. This improvement might correspond to a higher bacterial viability during sample preparation. For *E. coli*, only the initial glucose consumption was faster for samples with LB medium. However, for *B. subtilis*, the addition of LB medium generally increased consumption rates, reducing the glucose concentration at 24 h from 20 to 2%. Accordingly, the nutrients seem to provide a suitable environment and supply the cells during sample processing.

Long-term performance of bionanocomposites

Repeated testing cycles were carried out to evaluate bionanocomposite performance after multiple uses (Fig. 6).

For this purpose, after 24 h of glucose consumption with an initial concentration of 1 mg/mL, the bionanocomposites were rigorously washed with PBS to remove any remaining glucose and free bacteria. Subsequently, the composites were dried for 20 min and then transferred into fresh glucose media with a concentration of 1 mg/mL. This procedure was repeated after each 24 h consumption cycle. This was again investigated with and without the addition of LB medium.

Both *E. coli* and *B. subtilis* showed a decrease of cell viability after each cycle. Without the addition of LB medium, samples with *E. coli* could metabolize all glucose within just two cycles and its consumption gradually decreased after each cycle until the 6th day, when almost no glucose was metabolized anymore. In contrast, all glucose could be consumed up to the 6th day when LB medium was added to the composite. Besides that, it took approximately 6 days longer for the samples with LB medium to show similar residual concentrations of glucose and with that deterioration of their viability as the samples with no medium. Similar tendencies were observed with *B. subtilis*. Accordingly, for both bacteria, the addition of LB medium extended the timeframe for glucose consumption approximately six times. Based on these results, long-term performance of the embedded bacteria inside the ceramic during repeated test cycles could be confirmed.

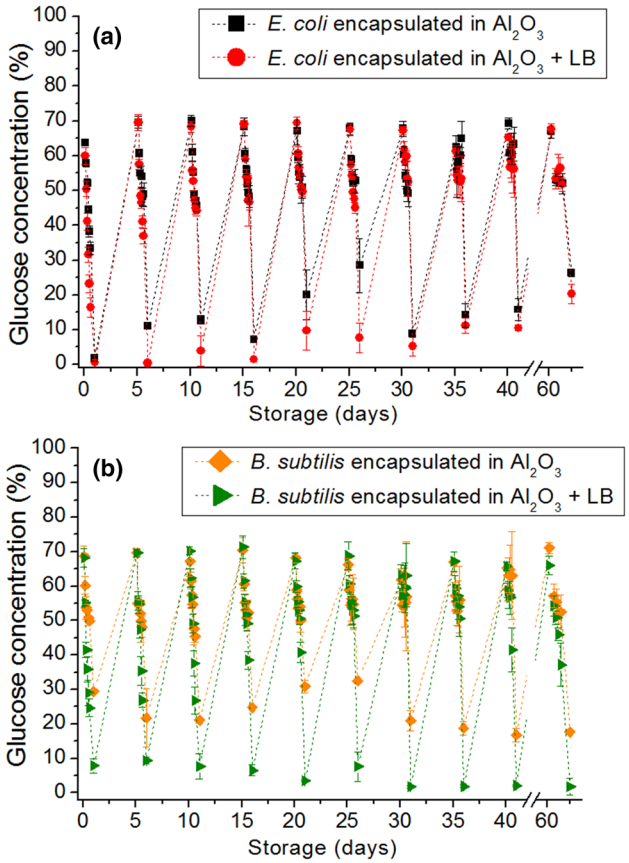

Fig. 7 Long-term stability of bionanocomposite with embedded *E. coli* (**a**) and *B. subtilis* (**b**) with and without the addition of LB medium stored in a refrigerator, measured by the glucose concentration over time

Long-term stability of bionanocomposites

To determine the long-term stability of the bionanocomposites, the embedded bacteria were stored, without being submersed in buffer solution, under sterile conditions at 4 °C. Glucose uptake was analyzed every 5 days with different samples, the results of which are depicted in Fig. 7. For samples produced with *E. coli*, a reduction of the bioactivity was observed with storage. After 60 days, remaining glucose concentrations of about 20 and 25% were observed for samples with and without addition of LB, respectively. The associated decrease of glucose consumption likely occurred gradually during storage and might be related to a reduction of the number of live cells. Samples with LB medium had a slightly higher glucose consumption after 60 days than samples without LB medium, the influence of LB medium being less significant for *E. coli*. Nevertheless, a reduction of just 20% of glucose from *E. coli* bioactivity after 60 days is a promising result, since the nanocomposite structure limits cell division or might otherwise negatively affect the microorganisms.

A different behavior was observed for the bionanocomposites with embedded *B. subtilis*. These samples did not show a reduction in glucose consumption, which might be explained by the capability of *B. subtilis* to undergo sporulation. Besides that, the influence of LB broth on cell viability was the same as for the cyclic tests (Fig. 4), which was constant during all cycles.

Conclusions

In summary, we showed that ceramic/hydrogel nanocomposites produced by ionotropic gelation are a suitable encapsulation matrix for bacteria. Electrostatic interactions of the negatively charged alginate and the positively charged alumina nanoparticles in combination with internal/external cross-linking increased compression strength four times as well as elastic modulus six times and resulted in a highly stable porous structure with low shrinkage and high water content. Furthermore, embedded bacteria viability increased approx. five times for *E coli* and three times for *B. subtilis* by just adding LB medium during processing. In addition, immobilized bacteria showed high glucose consumption which was comparable to non-immobilized cells. Additionally, adding LB medium to the bionanocomposites also increased glucose consumption for both bacteria. The

long-term performance of embedded bacteria was examined by performing repeated cycles of glucose consumption. Both bacteria *E. coli* and *B. subtilis* showed a gradual decrease of cell viability after each cycle. For both bacteria, the addition of LB medium extended the timeframe for glucose consumption approximately six times. Moreover, in long-term experiments, the embedded *E. coli* showed a gradual decrease of cell viability during storage up to a reduction 25% on glucose consumption capacity after 60 days. Conversely, storage did not significantly influence embedded *B. subtilis* performance during 60 days. These results demonstrate the great potential of this approach for producing bioactive composite materials for applications in bioprocessing.

Acknowledgements We would like to thank DFG Research Training Group GRK 1860, 'Micro-, meso- and macroporous nonmetallic materials: fundamentals and applications' (MIMENIMA) for funding.

Compliance with ethical standards

Conflict of interest The authors declare that they have no conflict of interest.

References

1. Dash HR, Das S (2012) Bioremediation of mercury and the importance of bacterial mer genes. Int Biodeterior Biodegrad 75:207–213
2. Dixit R et al (2015) Bioremediation of heavy metals from soil and aquatic environment: an overview of principles and criteria of fundamental processes. Sustainability 7(2):2189
3. Kang C-H, Kwon Y-J, So J-S (2016) Bioremediation of heavy metals by using bacterial mixtures. Ecol Eng 89:64–69
4. Han D et al (2013) Bacterial biotransformation of phenylpropanoid compounds for producing flavor and fragrance compounds. J Korean Soc Appl Biol Chem 56(2):125–133
5. Quintana MG, Dalton H (1999) Biotransformation of aromatic compounds by immobilized bacterial strains in barium alginate beads. Enzyme Microb Technol 24(3):232–236
6. Heipieper HJ et al (2007) Solvent-tolerant bacteria for biotransformations in two-phase fermentation systems. Appl Microbiol Biotechnol 74(5):961–973
7. Dien BS, Cotta MA, Jeffries TW (2003) Bacteria engineered for fuel ethanol production: current status. Appl Microbiol Biotechnol 63(3):258–266
8. Leroy F, De Vuyst L (2004) Lactic acid bacteria as functional starter cultures for the food fermentation industry. Trends Food Sci Technol 15(2):67–78
9. Anal AK, Singh H (2007) Recent advances in microencapsulation of probiotics for industrial applications and targeted delivery. Trends Food Sci Technol 18(5):240–251
10. Huq T et al (2013) Encapsulation of probiotic bacteria in biopolymeric system. Crit Rev Food Sci Nutr 53(9):909–916
11. Zhang B-B et al (2016) Robust and biocompatible hybrid matrix with controllable permeability for microalgae encapsulation. ACS Appl Mater Interfaces 8(14):8939–8946
12. Kang A et al (2014) Cell encapsulation via microtechnologies. Biomaterials 35(9):2651–2663
13. Gombotz WR, Wee SF (2012) Protein release from alginate matrices. Adv Drug Deliv Rev 64(Suppl):194–205
14. Das M, Adholeya A (2015) Potential uses of immobilized bacteria, fungi, algae, and their aggregates for treatment of organic and inorganic pollutants in wastewater. In: Water challenges and solutions on a global scale, chap 15, pp 319–337. https://doi.org/10.1021/bk-2015-1206.ch015
15. Böttcher H, Soltamnn U, Mertigb M, Pompe W (2004) Biocers: ceramics with incorporated microorganisms for biocatalytic, biosorptive and functional materials development. J Mater Chem 14:2176–2188
16. Martín MJ et al (2015) Microencapsulation of bacteria: a review of different technologies and their impact on the probiotic effects. Innov Food Sci Emerg Technol 27:15–25
17. de Vos P et al (2014) Polymers in cell encapsulation from an enveloped cell perspective. Adv Drug Deliv Rev 67–68:15–34
18. Orive G et al (2015) Cell encapsulation: technical and clinical advances. Trends Pharmacol Sci 36(8):537–546
19. Riddle KW, Mooney DJ (2004) Fundamentals of cell immobilisation biotechnology. Springer-Science + Business Media, B.V, New York, pp 22–26
20. Fedorovich NE et al (2011) Organ printing: the future of bone regeneration? Trends Biotechnol 29(12):601–606
21. Pillay V et al (1998) Ionotropic gelation: encapsulation of indomethacin in calcium alginate gel discs. J Microencapsul 15(2):215–226
22. Chan LW, Lee HY, Heng PWS (2006) Mechanisms of external and internal gelation and their impact on the functions of alginate as a coat and delivery system. Carbohyd Polym 63(2):176–187
23. Leong J-Y et al (2016) Advances in fabricating spherical alginate hydrogels with controlled particle designs by ionotropic gelation as encapsulation systems. Particuology 24:44–60
24. Sonego JM et al (2016) Ca(II) and Ce(III) homogeneous alginate hydrogels from the parent alginic acid precursor: a structural study. Dalton Trans 45(24):10050–10057
25. Haraguchi K (2007) Nanocomposite hydrogels. Curr Opin Solid State Mater Sci 11(3):47–54
26. Haraguchi K, Takehisa T, Fan S (2002) Effects of clay content on the properties of nanocomposite hydrogels composed of poly(*N*-isopropylacrylamide) and clay. Macromolecules 35(27):10162–10171
27. Kopeček J (2007) Hydrogel biomaterials: a smart future? Biomaterials 28(34):5185–5192
28. Thamaraiselvi TV, Rajeswari S (2004) Biological evaluation of bioceramic materials—a review. Trends Biomater Artif Organs 18:9–17
29. Warashina H et al (2003) Biological reaction to alumina, zirconia, titanium and polyethylene particles implanted onto murine calvaria. Biomaterials 24(21):3655–3661
30. Zhao F et al (2015) Composites of polymer hydrogels and nanoparticulate systems for biomedical and pharmaceutical applications. Nanomaterials 5(4):2054
31. Carrow JK, Gaharwar AK (2015) Bioinspired polymeric nanocomposites for regenerative medicine. Macromol Chem Phys 216(3):248–264
32. Song F et al (2015) Nanocomposite hydrogels and their applications in drug delivery and tissue engineering. J Biomed Nanotechnol 11(1):40–52
33. Blondeau M, Coradin T (2012) Living materials from sol–gel chemistry: current challenges and perspectives. J Mater Chem 22(42):22335–22343
34. Perullini M et al (2015) Alginate/porous silica matrices for the encapsulation of living organisms: tunable properties for biosensors, modular bioreactors, and bioremediation devices. Mesoporous Biomater 2:3–12
35. Pannier A et al (2012) Biological activity and mechanical stability of sol–gel-based biofilters using the freeze-gelation technique for

immobilization of *Rhodococcus ruber*. Appl Microbiol Biotechnol 93(4):1755–1767
36. Perullini M et al (2005) Cell growth at cavities created inside silica monoliths synthesized by sol–gel. Chem Mater 17(15):3806–3808
37. Perullini M et al (2011) Improving silica matrices for encapsulation of *Escherichia coli* using osmoprotectors. J Mater Chem 21(12):4546–4552
38. Carro L, Hablot E, Coradin T (2014) Hybrids and biohybrids as green materials for a blue planet. J Sol Gel Sci Technol 70(2):263–271
39. Brandes C et al (2014) Gel casting of free-shapeable ceramic membranes with adjustable pore size for ultra- and microfiltration. J Am Ceram Soc 97(5):1393–1401
40. Kuo CK, Ma PX (2001) Ionically crosslinked alginate hydrogels as scaffolds for tissue engineering: part 1. Structure, gelation rate and mechanical properties. Biomaterials 22(6):511–521
41. Growney Kalaf EA et al (2016) Characterization of slow-gelling alginate hydrogels for intervertebral disc tissue-engineering applications. Mater Sci Eng C 63:198–210
42. Smidsrød O, Skjåk-Braek G (1990) Alginate as immobilization matrix for cells. Trends Biotechnol 8:71–78
43. Groboillot A, Boadi DK et al (1994) Immobilization of cells for application in the food industry. Crit Rev Biotechnol 14(2):75–107
44. Bajpai SK, Kirar N (2016) Swelling and drug release behavior of calcium alginate/poly (sodium acrylate) hydrogel beads. Des Monomers Polym 19(1):89–98
45. Lin Z et al (2019) 3D printing of mechanically stable calcium-free alginate-based scaffolds with tunable surface charge to enable cell adhesion and facile biofunctionalization. Adv Funct Mater. https://doi.org/10.1002/adfm.201808439